Design and Development of Novel Micromachined Patch Antennas for Wireless Applications

Eve Y. Tsai, Andrew M. Bacon, Manos Tentzeris, and John Papapolymerou

School of Electrical and Computer Engineering, Georgia Institute of Technology, Atlanta, GA 30332, USA
Phone: 1-404-894-7516, Fax: 1-404-894-0560, Email: gt3592a@prism.gatech.edu

Abstract — **Results from the design and development of novel micromachined patch antennas on silicon are presented in this paper. These structures include a thin layer of low permittivity material (SiO_2, polyimide) between the antenna and the silicon substrate. The effect of the geometrical dimensions, the feeding configuration and the choice of the dielectric of the thin layer on the antennas' performance is also extensively discussed and preliminary design rules are derived.**

1. Introduction

Microstrip antennas are commonly used in wireless applications due to the fact that can be planar or conformal, can be fed in numerous configurations and also are compact and suitable for antenna array designs. In general, they can be used in applications requiring high-performance compact low-cost planar antennas. One of the main limitations of the microstrip antennas is the excitation of surface waves in the silicon substrate especially in cases where the bandwidth and the radiation efficiency requirements demand large values of the substrate thickness.

While high-dielectric constant substrates provide the capability of small-size circuit, micromachining techniques can locally synthesize a low-dielectric antenna substrate. In addition, the low-resistivity Si wafer used for traditional microwave circuit is troublesome due to the high loss [1] – [4].

In this paper, a micromachining approach that allows to etch a shallow cavity directly under the area of microstrip antenna, and then fills the cavity with lower permittivity materials, such as silicon dioxide or polyimide, is presented. A metal layer is deposited between the low permittivity material and the silicon underneath. The thin layer of low permittivity substrate can reduce the loss and the excitation of surface waves. The tradeoff is that the very small thickness of this layer makes the realization of practical bandwidths for this type of microstrip antennas very difficult. Finding the most efficient thickness, in term of fabrication feasibility and bandwidth of the antenna, is the most critical problem of these designs.

One important factor of the antenna performance is the choice of the optimum feeding options. Microstrip antennas are usually fed with either probe, CPW or microstrip feed. The radiating structures of this paper use a coplanar waveguide (CPW) feed to the microstrip antenna [5], in order to minimize the interaction of the coplanar mode fields with the lossy Si substrate. The latter will prevent loss of power in the feeding network. A short CPW-to-microstrip transition is also used to facilitate the patch feeding. In addition, CPW interfaces very well with the pad-probes of most measurement equipment. To integrate the microstrip antenna in the CPW feeding network, a simple, low-loss, compact and via-less CPW to microstrip transition was designed and optimized for operation around 30GHz.

2. Background

The material used in our designs was a Silicon substrate with relative permittivity (ε_r) of 11.8, conductivity (σ) of 100 S/m and thickness of 500μm at 30 GHz. With these high values of thickness and conductivity, it was assumed that the substrate provided a virtual ground, below which the E-field would be less than 5% of the E-field on the antenna. The attenuation constant (α) for such a material can be calculated with

$$\alpha = \omega\sqrt{\frac{\mu\varepsilon'}{2}\left(\sqrt{1+\left(\frac{\varepsilon''}{\varepsilon'}\right)^2}-1\right)}$$

where $\varepsilon'=\varepsilon_r\varepsilon_0$ and $\varepsilon''=\sigma/\omega$, giving a value of α=3120.41 Np/m for the above Silicon substrate. Using this attenuation constant in the formula

$$|E(z)| = |E_0|\, e^{-\alpha z}$$

the electric field left at the bottom of the silicon is approximately 21.01% of the electric field on top [6]. This means that there is still energy left at the bottom of the substrate, that excites significant substrate modes and could potentially distract the radiation of the antenna, unless a metal plane is added to the bottom.

3. Micromachined Antenna

To alleviate this problem, a shallow cavity was etched directly under the area of microstrip antenna, and then filled with lower permittivity materials, such as silicon dioxide or polyimide. A metal layer was added at the horizontal planar interface between the low permittivity material and the silicon underneath. Figure 1 shows the top view of this antenna. Figure 2 and 3 are the side views of the antenna with SiO_2 and polyimide underneath, respectively. The entire structure, including CPW, microstrip line, and the patch antenna are on top of the cavity. The CPW and microstrip line are designed to match a 50Ω characteristic impedence.

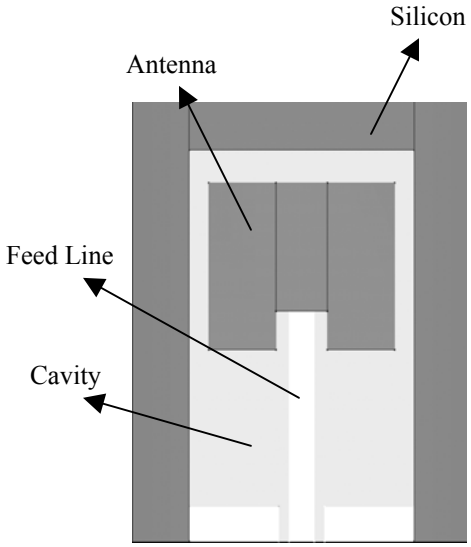

Fig.1 Top View of Antenna

The thickness of the cavity depends on the material used to fill the cavity. The dimension of the antenna is 3300μm by 2600μm. To match the 50Ω input impedence, the antenna is fed at 600μm from the edge. The width of the microstrip transmission line is 452μm and the distance from the edge of the antenna to the end of the cavity is 350μm on the side and 511.3μm in the front.

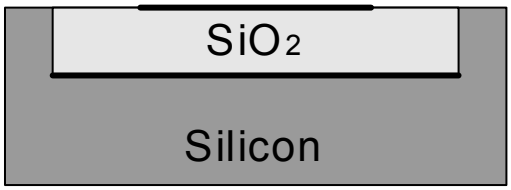

Fig.2 Antenna with SiO_2

The SiO_2 has ε_r = 3.5. The cavity depth with SiO_2 filling has been simulated at 50μm, 100μm, and 200μm. The bottom of the cavity is metalized with gold.

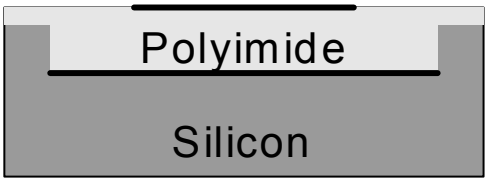

Fig.3 Side View of Antenna with Polyimide

The polyimide has ε_r = 3.2. During the fabrication, the polyimide is applied using a spin coating method that results in an extra layer of polyimide over the cavity and the silicon. The depths of the cavity that are simulated are equal to 50 μm, 100μm and 200μm. To derive the simulation results, we used a Finite-Difference Time-Domain (FDTD) code developed in-house and the *Microstripes* Antenna CAD tool.

4. Results

A. SiO_2

For SiO_2 layers, the thicknesses are 50μm, 100μm, and 200μm. Table 1 summarizes the result of each design simulation, and Figure 4 is a graphical presentation of the S11 values versus frequency for the three different simulated structures.

Table 1 SiO_2 Filled Cavity with Different Thickness

SiO_2 Thickness (μm)	Resonant Frequency (GHz)	Band-width (%)	Directivity (dBi)
50	28.946	1.4	6.736
100	29.165	1.7	6.766
200	29.430	2.4	6.809

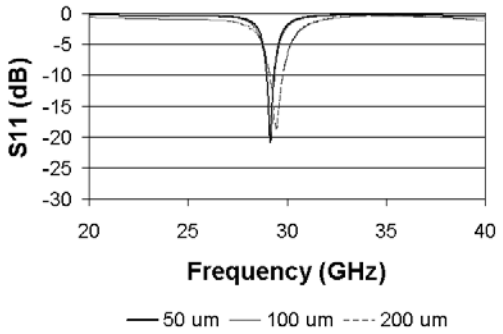

Fig.4 Simulated S_{11} for SiO_2 cavity

All three designs show a resonant frequency around 30GHz. The curve for 50μm and 100μm are almost identical with only 0.3% difference of the bandwidth. The 200μm design shows more bandwidth, but the maximum return loss is slightly higher than for the thinner layers. The 200μm design is the only one having a bandwidth close to the commonly required value of 3%. However, fabrication of the 200μm design is difficult, since growing such large oxidation thicknesses on silicon is very time-consuming and technologically challenging.

B. Polyimide

The polyimide structure is also simulated with three different thicknesses: 50μm, 100μm and 200 μm. Table 2 and Figure 5 summarize the results from simulation.

Table 2 Polyimide Filled Cavity with Different Thickness

Polyimide Thickness (μm)	Resonant Frequency (GHz)	Band-width (%)	Directivity (dBi)
50	30.318	1.3	6.616
100	29.474	1.3	7.223
200	30.975	2.7	6.809

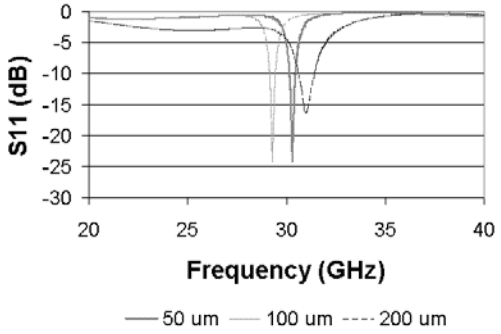

Fig.5 Simulated S_{11} for Polyimide cavity.

At 30.975GHz, the 200μm design has a return loss of 16.5dB, and a bandwidth of 2.7% (83.63MHz). As conclusion, the simulation results show that with 200μm of polyimide, both the resonant frequency and the bandwidth are in a desirable range.

C. SiO_2 Versus Polyimide

Figure 6 is a plot of S11 for the structures with 200μm of material, both SiO_2 and Polyimide. It can be easily observed that there is a shift of the resonant frequency for the two substrates. This is due to the fact that the polyimide has an extra layer on top of silicon that creates a cavity of a non-canonical shape. In addition, this introduces a dielectric interface of Z-shape in comparison to the dielectric interface of L-shape for SiO_2 (Figures 2 and 3), leading to a slightly lower value of effective dielectric constant and thus to a higher resonant frequency for the same physical dimensions.

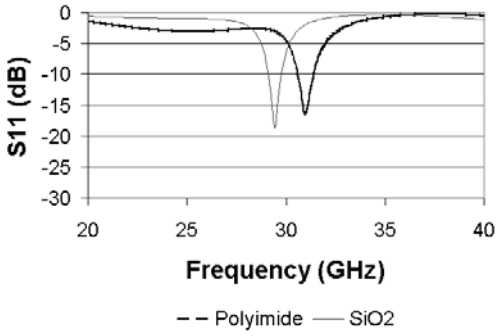

Fig.6 Simulated S_{11} for the Same Thickness (200μm) of SiO_2 and Polyimide

Both simulations demonstrate a bandwidth of approximately around 2.5%. SiO_2 shows better return loss at the resonant frequency, though it is more difficult to fabricate. On the contrary,

Polyimide-filled geometry is more feasible in terms of fabrication.

In order to decrease the difference between the resonant frequencies of the SiO_2 and polyimide antennas, we redesigned the latter one. The size of the antenna was changed from 3300μm by 2600μm to 3300μm by 2650μm. The result shows a maximum return loss of 29.09dB at 30.022GHz, and the bandwidth is 2.7%. Figure 7 shows the comparison from this optimized dimension to the SiO_2 result. The central bandwidth is offset by 600MHz, which is 2%. The difference can be attributed to different dielectric constants and numerical errors due to the simulation tools.

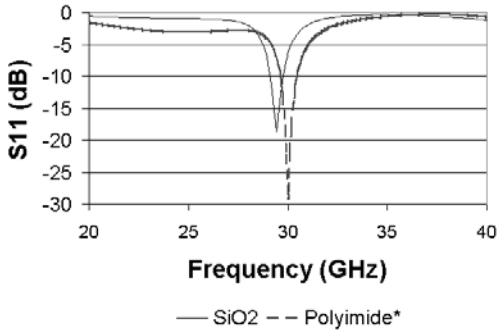

Fig.7 Simulated S11 for Same Thickness (200μm) of SiO_2 Revised Polyimide

5. Conclusion

In this paper, preliminary designs of planar antenna structures on top of low resistivity silicon with a layer of low permittivity material in between are presented and evaluated in terms of return loss and bandwidth. The materials used are SiO_2 and Polyimide and simulation results show that to achieve bandwidths above 2.5%, it is necessary to have at least 200μm of either material. Polyimide is easier to fabricate, but SiO_2 could provide a better performance in terms of the return loss. Future work in this area will involve the investigation of different low-ε_r materials and fabrication processes, as well the evaluation of the radiation patterns.

ACKNOWLEDGEMENT

The authors wish to acknowledge the support of the NSF under Career Award# 9984761 and SGER Award# 0196376, the Yamacraw Design Center of the State of Georgia and the Georgia Tech Packaging Research Center. In addition, they would like to thank Ms. Emily Zheng for the information she provided about the micromachining and the fabrication processes.

REFERENCE

[1] J. Papapolymerou, C. Schwartzlow, G Ponchak, "A Folded-Slot Antenna on Low Resisitivity Si Substrate with a Polyimide Interface Layer For Wireless Circuit," *Silicon Monolithic Integrated Circuits in RF Systems, 2001*, pp. 215 –218

[2] J.P.Papapolymerou, R.F.Drayton and L.P.B.Katehi, "Micromachined Patch Antennas", IEEE Trans. Antennas and Propagation, vol.46, pp.275-283, Feb.1998.

[3] G.Gauthier, J.-P.Raskin, L.P.B.Katehi and G.M.Rebeiz, "A 94-GHz Aperture-Coupled Micromachined Microstrip Antenna", IEEE Trans. On Antennas and Propagation, Vol.47, No.12, pp.1761-1766, Dec.1999.

[4] G.P.Gauthier, A.Courtay and G.M.Rebeiz, "Microstrip Antennas on synthesized low dielectric-constant substrates", IEEE Trans. Antennas and Propagation, vol.45, pp.1310-1314, Aug.1997.

[5] G. Gauthier, L. P. Katehi, G. M. Rebeiz, "W-band finite ground coplanar waveguide (FGCPW) to microstrip line transition," *Porc. 1998 IEEE Symposium on Microwave Theory and Techniques*, pp. 107- - 109.

[6] F. Ulaby, *Fundamentals of Applied Electromagnetics*, Prentice Hall, Upper Saddle River, New Jersey, 1999.